



## Original article

## Magnetic metal organic framework for pre-concentration of ampicillin from cow milk samples

Ahmad Reza Bagheri, Mehrorang Ghaedi\*

Chemistry Department, Yasouj University, Yasouj, 75918-74831, Iran

## ARTICLE INFO

## Article history:

Received 14 September 2019

Received in revised form

2 January 2020

Accepted 16 February 2020

Available online 20 February 2020

## Keywords:

Magnetic metal organic framework  
Ultrasound assisted magnetic solid phase  
extraction

Ampicillin

Cow milk samples

## ABSTRACT

The aim of this study is a present of a simple solvothermal synthesis approach to preparation of Cu-based magnetic metal organic framework (MMOF) and subsequently its application as sorbent for ultrasound assisted magnetic solid phase extraction (UAMSPE) of ampicillin (AMP) from cow milk samples prior to high performance liquid chromatography-Ultraviolet (HPLC-UV) determination. Characteristics of prepared MMOF were fully investigated by different techniques which showed the exclusive properties of proposed sorbent in terms of proper functionality, desirable magnetic property and also high specific surface area. Different influential factors on extraction recovery including sorbent dosage, ultrasonic time, washing solvent volume and eluent solvent volume were assessed using central composite design (CCD) based response surface methodology (RSM) as an operative and powerful optimization tool. This is the first report for determination of AMP using MMOF. The proposed method addressed some drawbacks of other methods and sorbents for determination of AMP. The presented method decreases the extraction time (4 min) and also enhances adsorption capacity (250 mg/g). Moreover, the magnetic property of presented sorbent (15 emu/g) accelerates the extraction process which does not need filtration, centrifuge and precipitation procedures. Under the optimized conditions, the proposed method is applicable for linear range of 1.0–5000.0 µg/L with detection limit of 0.29 µg/L, satisfactory recoveries ( $\geq 95.0\%$ ) and acceptable repeatability (RSD less than 4.0%). The present study indicates highly promising perspectives of MMOF for highly effective analysis of AMP in complicated matrices.

© 2020 Xi'an Jiaotong University. Production and hosting by Elsevier B.V. This is an open access article under the CC BY-NC-ND license (<http://creativecommons.org/licenses/by-nc-nd/4.0/>).

## 1. Introduction

AMP is a semisynthetic antibiotic which belongs to penicillin groups. It generally has been applied for treatment of bacterial infections caused by both gram-positive and gram-negative bacteria in both humans and animals [1]. AMP acts by inhibiting the proteinsynthesis of the bacterial cell wall. It is comparatively less toxic than other antibiotics, and side effects are more likely in those who are sensitive to penicillins and those with a history of asthma or allergies. In very rare cases, it causes severe side effects such as angioedema, anaphylaxis, and *C. difficile* infection. In addition, it can cause stomach cramps, diarrhea, dizziness, nausea, rashes and peeling of the skin when consumed by humans [2]. AMP overdose can cause behavioral changes, confusion, blackouts, and convulsions, as well as neuromuscular hypersensitivity, electrolyte imbalance, and renal failure. The maximum residue limits (MRLs)

for ampicillin in milk and meat have been set by the European Union (EU) at 40 and 50 µg/kg, respectively [3]. In 1999, the EU forbade the use of antibiotics as additives in animal feed, but they are still use in some countries. Therefore, considerable interest has been devoted to monitoring and determination of AMP in different samples, especially cow milk samples. On the other hand, cow milk samples contain complicated matrices such as proteins, hormones, and long chain fatty acids which can significantly pollute chromatography column and/or overlap with peak of AMP during quantitative analysis of AMP (in chromatographic determination). Hence, for the detection of AMP at trace level, the fundamental steps can be attributed to the sample clean-up in order to eliminate complicated matrices and also pre-concentrate AMP in cow milk samples. Up to date, different sample preparation approaches have been applied for determination of AMP, among which solid phase extraction (SPE) has been paid much interest to due to its exclusive properties in terms of easy operation, low analysis cost and easy automation [4]. Although different sorbents have been used in SPE, some of them have some limitations including low physical and chemical stability, hardness to modification, low specific surface

Peer review under responsibility of Xi'an Jiaotong University.

\* Corresponding author.

E-mail address: [m\\_ghaedi@mail.yu.ac.ir](mailto:m_ghaedi@mail.yu.ac.ir) (M. Ghaedi).

area and also low adsorption capacity. To address these drawbacks, metal organic frameworks (MOFs) are very much preferred. MOFs are porous materials with high specific surface area which is achieved based on the coordination interactions between metal cations (clusters or secondary building units) and organic ligands (linkers) via coordinative bonds [5]. They have aroused great interest principally due to their versatility, diverse structures, tunable porosity and specific surface area, ease of functionalization, unsaturated metal sites, and also biocompatibility [6]. Among the MOFs, copper-based MOFs particularly draw great attention because they can be synthesized with available commercially reagents and possess high surface area [7]. The strong Cu (II)–O bonds from copper metal nodes and organic ligands endow Cu-MOFs with excellent stability in aqueous solution over a wide pH range. Cu based MOFs draw interest in many areas due to their unique structure which is made an interconnected channel of square-shaped pores (9 Å by 9 Å) [8]. It is noteworthy that in spite of all SPE benefits, it is faced with some main drawbacks such as long extraction time and also consumption of large volume of solvents, which forced researchers to use an alternative method. Magnetic solid phase extraction (MSPE) is a versatile technique in which samples are gathered using an external magnetic field without using filtration, centrifuge and precipitation procedures. In addition, MSPE does not need high volume of organic solvent or conditioning the sorbent and column packing elimination [5,9], which not only decreases extraction time but also enhances the contact surface area and also repeatability [10]. Ultrasound irradiation can accelerate chemical process which can be attributed to formation of microbubbles via sound waves through the solution [11,12]. Formation of bubbles in solution can accelerate and improve mass transfer process that can be related to best immersion of sorbent in bulk solution and also strong enhancement of diffusion coefficient [13]. Hence, in this study, we synthesized Cu based MMOF through a simple and facile solvothermal method and applied it as sorbent for the first time for UAMSPE of AMP from cow milk samples. The performance of the proposed method was assessed using CCD based RSM in order to minimize experimental runs, time, chemicals consumption, reagents, and attain more accurate results. The prepared MMOF was fully characterized and the effects of influential factors on extraction were also evaluated. In addition, under the optimized conditions, the fully validated developed method was applied for the analysis of AMP in different cow milk samples.

## 2. Experimental

### 2.1. Materials and instruments

AMP pure powder was obtained from the Ministry of Health and Medical Education (Tehran, Iran). Iron (III) chloride hexahydrate ( $\text{FeCl}_3 \cdot 6\text{H}_2\text{O}$ ), iron (II) chloride tetrahydrate ( $\text{FeCl}_2 \cdot 4\text{H}_2\text{O}$ ), ammonium hydroxide ( $\text{NH}_4\text{OH}$ ), Cu (II) nitrate trihydrate  $\text{Cu}(\text{NO}_3)_2$ , terephthalic acid ( $\text{H}_2\text{BDC}$ ), tetrahydrofuran (THF), NaOH, HCl, ethanol, methanol, hexane, acetone, and acetonitrile (HPLC grade) were purchased from Merck (Darmstadt, Germany). Ultrapure water was prepared from a MilliQ gradient water purification system. Fourier transform infrared spectroscopy (FT-IR-8300, Shimadzu) via KBr pellet was used to give an idea about MMOF functional groups. Morphology of prepared MMOF was examined by scanning electron microscope (SEM) (SIGMA VP microscope from ZEISS, Germany). Transmission electron microscopy (TEM) image on a Hitachi S-570 microscope from Hitachi (Tokyo, Japan) was applied for investigation of the structure of prepared MOF. X-ray diffraction (XRD, Philips PW 1800) was performed to characterize the phase and structure of the prepared MOF using  $\text{Cu}_{\text{K}\alpha}$  radiation (40 kV and 40 mA) at angles ranging from  $5^\circ$  to  $80^\circ$ . Vibrating

sample magnetometer (VSM) (LDJ 9600-1, USA) was employed to evaluate the magnetic property of MMOF. The Brunauer–Emmett–Teller (BET) surface area was calculated from  $\text{N}_2$  adsorption-desorption isotherms at 77 K using a BELSORP Mini (Microtrac Bel Corp, USA). A Tecno GAZ SPA Ultra Sonic System (Parma, Italy) ultrasound bath was used at 130 W at 40 kHz frequency with a maximum of about 3 L of water throughout the experiment. A Metrohm 780 pH meter (Metrohm Co., Herisau, Switzerland) was used for monitoring the pH values. STATISTICA version 10.0 (Stat soft Inc., Tulsa USA) and Design-Expert version 7.0.0 software were used for experimental design analysis. AMP determination was done using an Agilent 1100 liquid chromatography system equipped with a micro vacuum degasser (model G1379A), a quaternary pump (model G1311A), a multiple wavelength detector (model G13658:220 nm for HCT), a sample injection valve with a 20  $\mu\text{L}$  of sample loop, and a Knauer  $\text{C}_{18}$  column (4.6 mm i. d.  $\times$  250 mm, 5  $\mu\text{m}$ ) at room temperature using mobile phase that consisted of acetonitrile:ammonium acetate (15:85, V/V) filtered through a 0.45  $\mu\text{m}$  filter, degassed under vacuum and passed with the flow rate of 0.7 mL/min. Separation process was carried out at ambient temperature and detector wavelength was set at 280 nm.

### 2.2. Synthesis of MMOF

First,  $\text{Fe}_3\text{O}_4$  nanoparticles were synthesized using chemical coprecipitation according to our previous work [9,10]. In the next step, 0.5 g of prepared  $\text{Fe}_3\text{O}_4$  nanoparticles were fully dispersed in 75 mL (DMF (40 mL): ethanol (35 mL)) under ultrasonic irradiation for 1 h. Then, 1 g  $\text{H}_2\text{BDC}$  and 4 g  $\text{Cu}(\text{NO}_3)_2$  were added to the mixture and dispersed uniformly. The mixture was transferred to a 100 mL polytetrafluoroethylene lined stainless steel autoclave and placed in an oven at  $120^\circ\text{C}$ . After 12 h, it was taken out and cooled down at room temperature. Then, the products were separated using an external magnet and washed several times with DMF and water. Finally, MMOF was obtained by drying the product in  $80^\circ\text{C}$  oven for 12 h.

### 2.3. Adsorption test

To investigate the adsorption capacity of MMOF, 30.0 mg of MMOF was dispersed in 15 mL of AMP solution with different concentrations (5.0–50.0 mg/L) by stirring for 30 min. To obtain the adsorption capacity of prepared MMOF, it was separated from solution by an external magnet and residual (non-sorbed) concentrations of AMP in the supernatant were analyzed by HPLC. The equilibrium adsorption capacity ( $Q$ , mg/g) of MMOF was calculated according to the following equation:

$$Q = \frac{(C_0 - C_t)V}{m} \quad (1)$$

where  $C_0$  (mg/mL) and  $C_t$  (mg/mL) are the initial and the supernatant concentration of AMP after adsorption, respectively;  $V$  (mL) is the sample solution volume and  $m$  is the mass of the MMOF.

### 2.4. Milk samples pre-treatment protocol, calibration standard preparation and MMOF-MSPE procedure for determination of AMP from cow milk samples

Fresh cow milk samples were collected from paddocks at (Shiraz, Iran). Cows had not received antibiotic treatment within the last 6 weeks. The protocol used for pretreatment of milk samples is detailed below. 20 mL of acetonitrile was added to 5 mL of cow milk sample to precipitate the proteins and placed in a refrigerator for

20 min to allow the interaction of the solvent with the sample and facilitate proteins and fat removal. The mixture was then centrifuged for 10 min at 12,000 rpm, resulting in a top layer of fat and a solid protein precipitation at the bottom. Fat was extracted by suction with the aid of a syringe and the supernatant containing the analyte was collected using a Pasteur Pipette and was used for MMOF-MSPE-HPLC/UV procedure. A standard AMP stock solution (100.0 mg/L) was prepared by dissolving 10.0 mg of AMP in 100.0 mL of deionized water and its subsequent appropriate dilution applied as working solution. Fig. 1A shows the MMOF-MSPE-HPLC/UV procedure for extraction of AMP from cow milk samples. In this regards, 15 mL of extracted cow milk sample solution with the AMP spiked concentration of 200.0  $\mu\text{g/L}$  was adjusted at pH 7.0 using HCl and NaOH and the solution was mixed with 30.0 mg of MMOF in the beaker under the ultrasound irradiation for 4.0 min. Subsequently, the MMOF was separated with an external magnet and eluted by 3 mL of acetone as washing solvent and subsequently with 3 mL of methanol: ethanol (50:50, V/V) as eluent. The eluent was evaporated to dryness under nitrogen stream in water bath (35 °C) and the residue was subsequently reconstituted in 100  $\mu\text{L}$  mobile phase (acetonitrile/ammonium acetate) (15:85, V/V) and 20  $\mu\text{L}$  of it ready for HPLC-UV analysis.

### 3. Results and discussion

#### 3.1. Synthesis and characterization of MMOF

The solvothermal synthesis process of MMOF is schematically shown in Fig. 1B. First,  $\text{Fe}_3\text{O}_4$  magnetic nanoparticles (MNPs) were synthesized by co-precipitation method. This method was selected to synthesis of  $\text{Fe}_3\text{O}_4$ -MNPs due to its exclusive properties in terms of less consumption of hazardous materials and an organic solvents compared to other methods [14].  $\text{Fe}_3\text{O}_4$  nanoparticles have Fe–O groups in which the oxygen groups have the ability to chelate with metal ions ( $\text{Cu}^{2+}$ ). Next, the conjugated central metal  $\text{Cu}^{2+}$ ,

$\text{H}_2\text{BDC}$  and  $\text{Fe}_3\text{O}_4$  were combined to form a MMOF material by simple solvothermal method. It is noteworthy that the preparation of common MMOF uses more complicated experimental equipment, more amounts of (toxic) reagents and higher temperature control. Happily, our synthesis method represents significant advantages of eco-friendliness, cost-savings, simplicity, rapidity and efficiency. The prepared MMOF was fully characterized by FT-IR, XRD, EDX, SEM, TEM, VSM and BET analyses as follows.

Fig. 2 presents the FT-IR spectra of  $\text{Fe}_3\text{O}_4$  (A), MOF (B) and MMOF (C), respectively. In Fig. 2A, the peak at  $578\text{ cm}^{-1}$  is related to Fe–O peak, and the broad peak around  $3400\text{ cm}^{-1}$  could be attributed to OH functional groups of  $\text{Fe}_3\text{O}_4$ . The Fe–O peak was also observed in MMOF with lower intensity which showed the successful decoration of  $\text{Fe}_3\text{O}_4$  nanoparticles with MOF (Fig. 2C). In Figs. 2B and C, the bands obtained at  $488\text{ cm}^{-1}$  and  $721\text{ cm}^{-1}$  may be due to the bending and stretching modes of Cu–O, respectively [15]. The observed peaks between  $663$  and  $766\text{ cm}^{-1}$  are assigned as ring in and out of plane bending vibration of aromatic ring of  $\text{H}_2\text{BDC}$ . In addition, aromatic carbon C–C vibrational mode resulted in the bands at about  $1390\text{ cm}^{-1}$  [16]. Also, the peaks at  $970\text{ cm}^{-1}$ ,  $1500\text{ cm}^{-1}$  and  $1640\text{ cm}^{-1}$  are related to C–O,  $-\text{C}=\text{C}-$  and  $\text{C}=\text{O}$  groups of  $\text{H}_2\text{BDC}$ , respectively [16]. The obtained results proved the successful synthesis of proposed materials.

Fig. 3A presents the XRD pattern of  $\text{Fe}_3\text{O}_4$  in which the peaks at  $2\theta$  of  $31.0^\circ$ ,  $35.5^\circ$ ,  $43.5^\circ$ ,  $53.0^\circ$ ,  $57.5^\circ$ ,  $62.5^\circ$  and  $74.0^\circ$  were corresponded to (220), (311), (400), (442), (511), (440) and (533) crystal planes [17]. Fig. 3B shows the XRD pattern of MOF in which the peaks at  $2\theta$  of  $7.0^\circ$ ,  $13.8^\circ$ ,  $15.7^\circ$ ,  $19.6^\circ$ ,  $30.0^\circ$ ,  $37.0^\circ$ ,  $42.5^\circ$ ,  $62.5^\circ$  and  $74.0^\circ$  are related to (220), (222), (333), (420), (422), (773), (882), (440) and (533) crystal planes respectively and are consistent with those in previous reported literature (Cambridge crystallographic information data with deposit number of 112,954) [15,18]. Fig. 3C presents the XRD pattern of MMOF which shows the related peaks, indicating that the crystalline structure of MOF was not changed and confirmed the successful synthesis of MMOF [19,20].

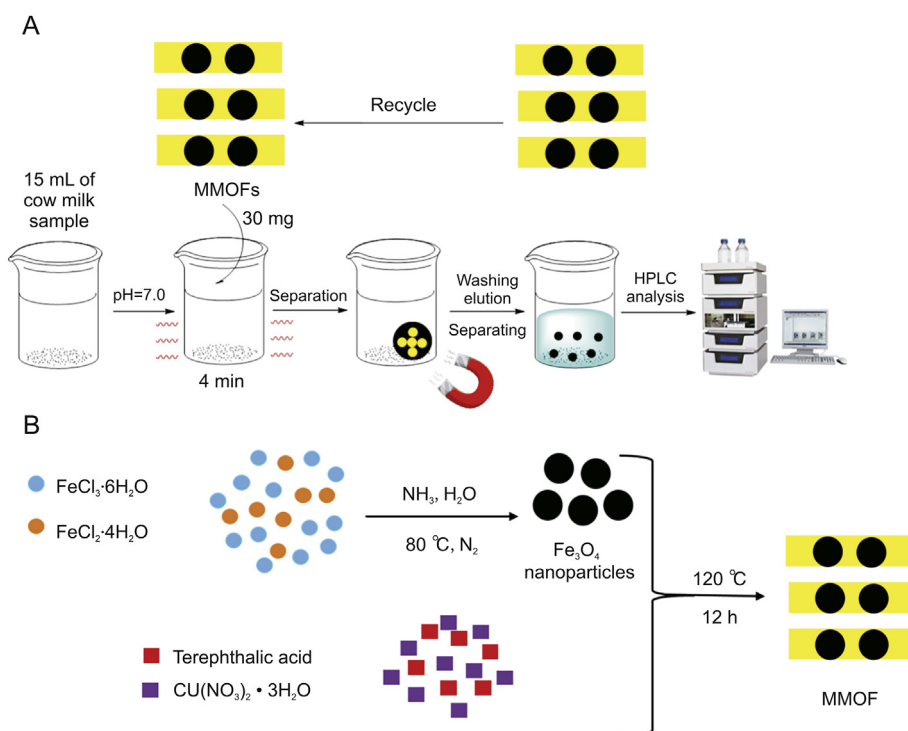


Fig. 1. The MMOF based MSPE procedure for ampicillin extraction (A) and the basic preparation procedure of MMOF (B).

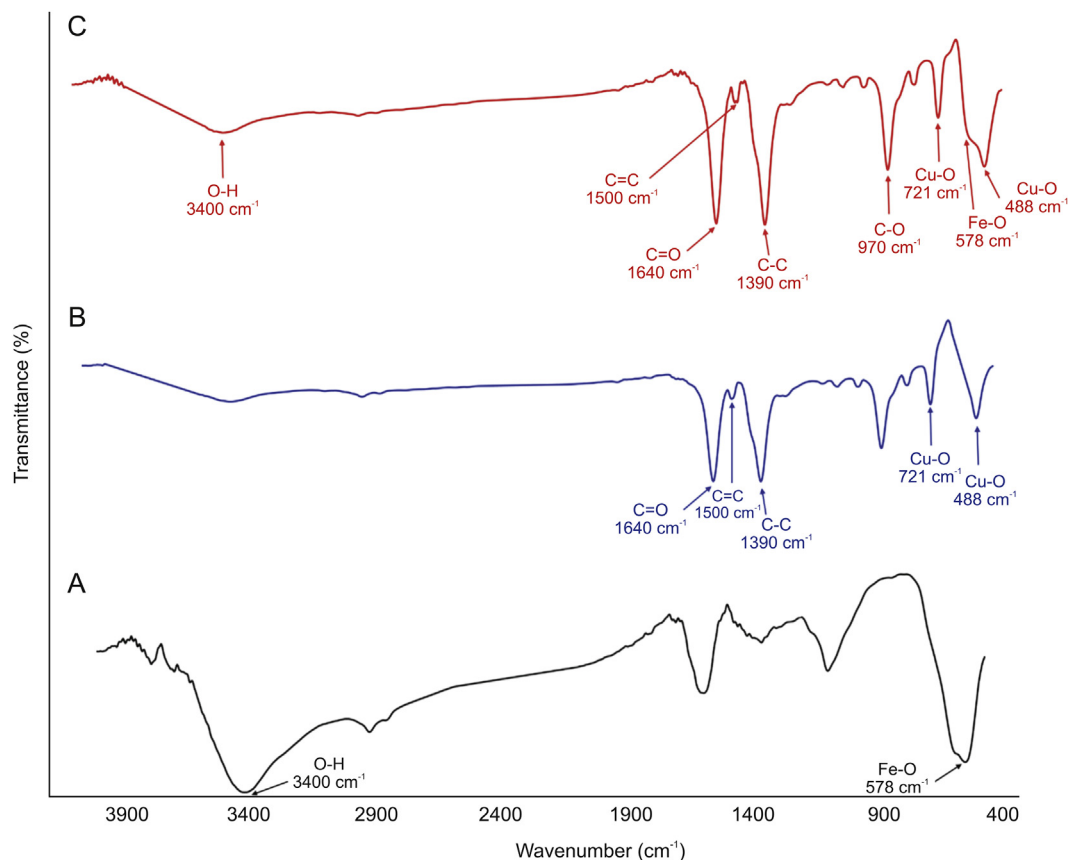


Fig. 2. The FT-IR spectra of  $\text{Fe}_3\text{O}_4$  (A), MOF (B) and MMOF (C).

Figs. 4A and B show the EDX analysis of MOF and MMOF respectively in which the presence of C, O and Cu elements in MOF and C, O, Cu and Fe elements in MMOF confirmed the successful synthesis of these materials.

SEM images of MOF (Figs. 4C and D) and MMOF (Fig. 4E) present the regular and ordered structure of MOF and composite structure of MMOF which provides a direct evidence for successful synthesis of the MMOF composites. The SEM image of prepared MOF is presented in different magnitude. Based on Figs. 4C and D, some of the prepared MOF is octahedral in shape while others are leaf-like sheets.

Fig. 5 shows the TEM images of prepared MMOF in which the dark region is related to  $\text{Fe}_3\text{O}_4$  nanoparticles and light region is related to MOF, which confirmed the successful preparation of MMOF. The TEM image proved the composite structure of prepared MMOF.

According to Figs. 6A and B, the magnetic saturation strength of  $\text{Fe}_3\text{O}_4$  and MMOF was 66.5 emu/g and 15 emu/g, respectively. The magnetic saturation strength of MMOF is higher than those in some other reports [21–23]. Seen from the picture in the bottom right of Fig. 6, the MMOF was dispersed in the water sample homogeneously and the turbid water sample could become clear quickly under an external magnetic field. Owing to high magnetic saturation strength, the MMOF could be easily isolated by wasting the least of energy without any complex equipment.

The specific surface area and porous structure of MOF and MMOF were checked by BET (Figs. 7A and B) and exhibited a type IV isotherm and strongly supported a mesoporous characteristic. The

specific surface area of MOF and MMOFs was achieved to be 400 and 300.00  $\text{m}^2/\text{g}$ , respectively. This case can be explained that  $\text{Fe}_3\text{O}_4$  particles partially filled the pores of MOF. In addition, pore sized distribution of MOF and MMOF were investigated and were obtained to be 10.64 nm and 5.35 nm, respectively. Porosity and high specific area of MMOF significantly facilitated mass transfer of AMP and the binding sites were more accessible to interact with AMP molecules.

### 3.2. Parameter optimization for UASPE based MMOF of AMP from cow milk samples

To attain maximum extraction yield of AMP in cow milk samples, the elementary effects of qualitative parameters such as pH and kind of washing and eluent solvents were evaluated at the spiked concentration level of 500.0  $\mu\text{g}/\text{L}$ .

The pH of solution can affect the ionic or neutrality structure of both AMP and MMOF and has a noticeable role in the extraction of AMP. In order to find the optimum pH value, the effect of sample pH was assessed in the range of 2.0–8.0, individually. Based on the structures of AMP and MMOF, the adsorption of AMP from cow milk samples by MMOF might be attributed to the combined action of hydrogen bonding,  $\pi$ - $\pi$  interaction, and also coordination bonds. On the other hand, we envisioned that the dominant adsorption mechanism is hydrogen bonding. Indeed, AMP has two pKas (2.5 and 7.3) [24] which are related to its carboxylic acid and amine functional groups, respectively. At pH value lower than 7.3, the amine group of AMP induces positive charge and changes to  $\text{NH}_3^+$ .

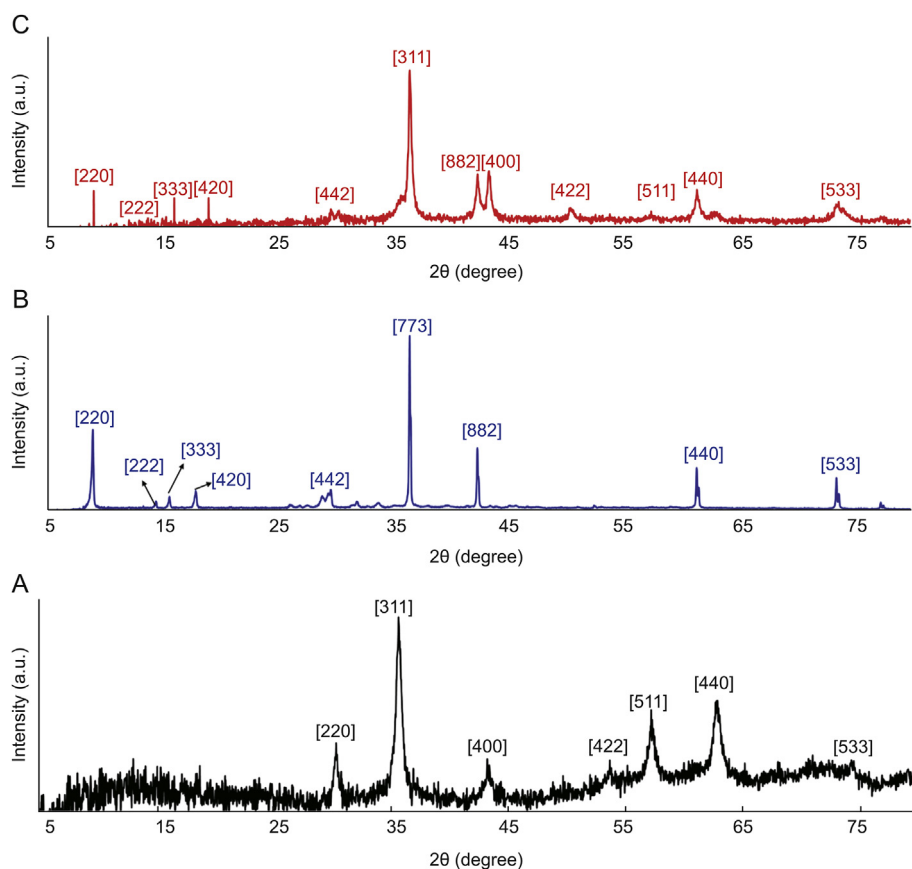


Fig. 3. The XRD pattern of  $\text{Fe}_3\text{O}_4$  (A), MOF (B) and MMOF (C).

On the other hand, in pH values between 2.5 and 7.3, the amine group is remained in  $\text{NH}_3^+$  form, while carboxylic groups get negative charge and transfer to carboxylate species. Also, at pH values higher than 7.3 the amine group and carboxylic groups remain in neutral and carboxylate forms, respectively. In pH values between 2.5 and 7.3, carboxylate groups of AMP can act as donor electrons and react with  $\text{Cu}^{2+}$  cations through coordination bonds while  $\text{COO}^-$  groups of  $\text{H}_2\text{BDC}$  can react with  $\text{NH}_3^+$  groups of AMP through hydrogen bonding. In addition, the adsorption of AMP by the MMOF can occur viz.  $\pi$ - $\pi$  interaction between benzene ring of AMP and  $\text{H}_2\text{BDC}$ . In the pH values between 2.5 and 7.3, due to the highest negative charge density and presence of utmost donor groups and also due to presence of amine group in  $\text{NH}_3^+$  form, we expected that the best recovery was obtained since experimental results confirm this phenomenon. Overall, at sample pH of 7.0, the maximum extraction recovery was achieved, which is logical (Fig. S1). Therefore, the sample pH of 7.0 was set for the rest of experiments.

Cow milk samples have complicated matrices such as proteins, hormones and other metabolites which not only can retain on MMOF and HPLC column but also can overlap with AMP peak and subsequently decrement the performance of the proposed method. Therefore, to decrease the effect of interfering species, different washing solvents with different polarity including deionized water, methanol, acetonitrile, acetone and hexane were examined to obtain the cleanest extracts. The results showed that the cleanest extraction was achieved when acetone was applied as washing solvent. This phenomenon could be related to rinsing strength of acetone as nonpolar solvent for washing nonpolar interferents while adsorbed AMP retains on MMOF.

Another key factor in MSPE is selection of eluent solvent which can completely desorb target analyte from sorbent. Hence, the effects of different eluents solvents as well as their mixture with different polarity including methanol, ethanol, acetonitrile and methanol:ethanol (50:50, V/V), were assessed. Experimental results confirmed that maximum extraction efficiency was achieved when methanol/ethanol (50:50, V/V) was applied as eluent and that this result might be due to the likeness between the polarity of AMP and methanol and ethanol and high rinsing strength of them.

### 3.3. CCD multivariate approach for assessment and optimization of an influential factors

Investigation and optimization of an effective factor on extraction recovery is a critical step in analytical methods which not only can monitor the effect of each factor individually but also can investigate the factor interactions as well as obtain true optimum levels. In this regard, different methods have been extensively applied for this purpose, among which one-factor-at-a-time (OFAT) is a common and popular approach in which the influence of one factor is monitored at a time, while other factors are fixed. In spite of simplicity and applicability, OFAT is faced with some main drawbacks such as a large number of experimental runs, labor effort, high consumption of chemicals and solvents, time consumption and high cost. Most importantly, it cannot distinguish the importance of parameters and their interactions and also it is unable to attain the true optimum levels. To address these obstacles, multivariate optimization techniques (MOT) are alternative methods in which the effects of several factors are evaluated concurrently. The reasons that distinguished MOT from OFAT are

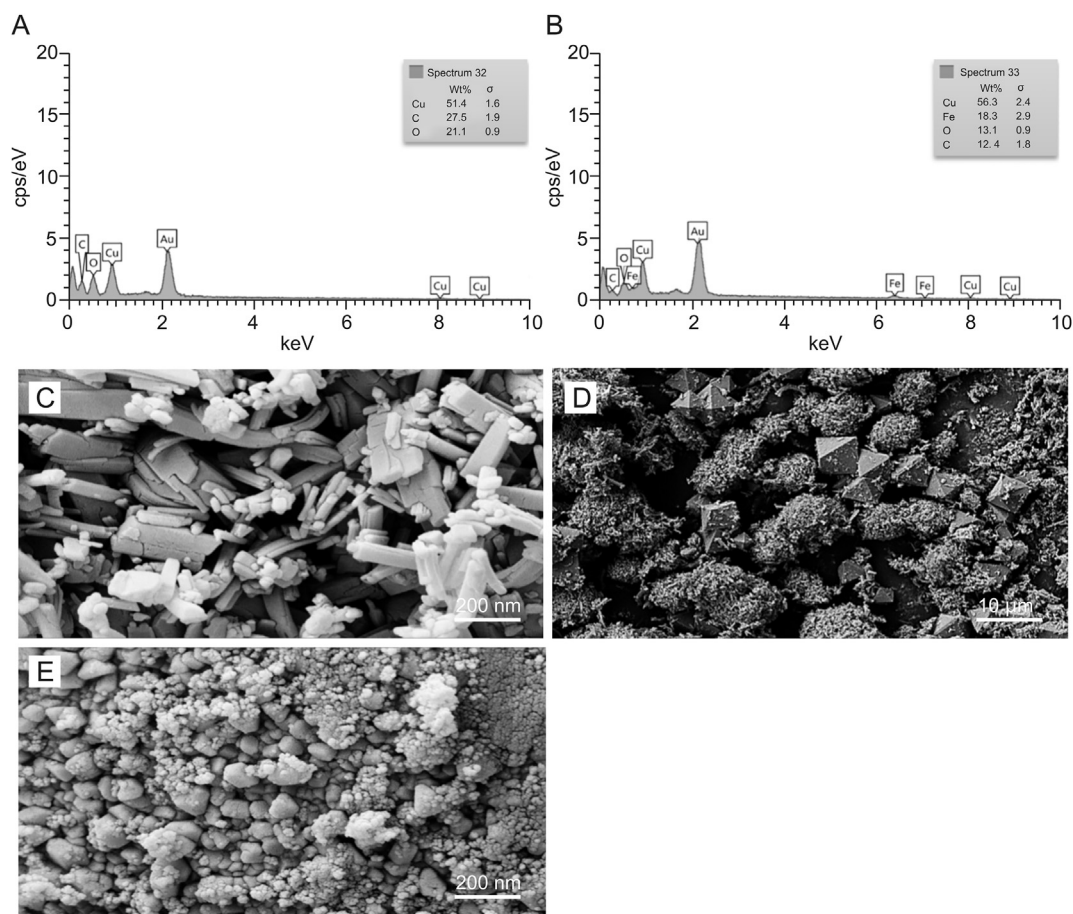


Fig. 4. EDX analysis of MOF (A) and MMOF (B) and SEM images of MOF (C and D) and MMOF (E).

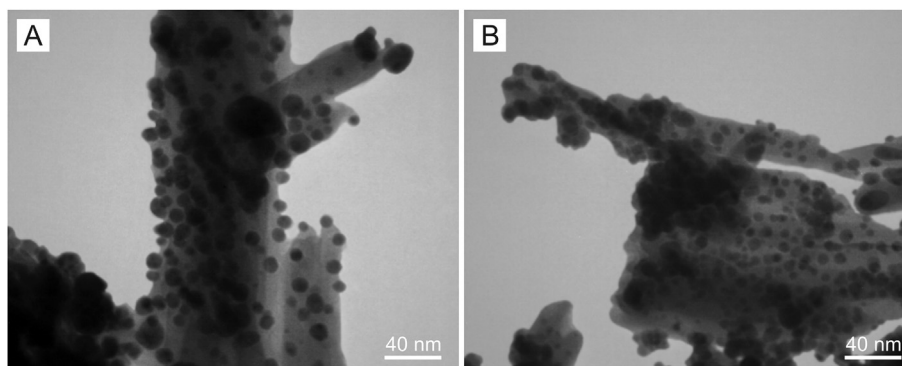


Fig. 5. TEM images of prepared MMOF.

that MOT can eliminate the drawbacks of OFAT and more interestingly MOT is able to estimate the interactions between different factors, yielding a more efficient optimization and also attaining the true optimum levels [25–28]. CCD based RSM is an efficient and powerful statistical and mathematical MOT that is able to evaluate the significance of factors, their interactions, relationships between target response and independent parameters, and most importantly it is able to attain the true optimum levels [29–32]. Therefore, in this work, the effects of four main qualitative factors such as MMOF dosage (A: 15.0–35.0 mg), ultrasonic time (B: 1.0–5.0 min), washing solvent volume (C: 1.5–3.5 mL) and eluent solvent volume (D: 1.5–3.5 mL) as well as their interactions affecting extraction

efficiency of AMP were performed through CCD based RSM according to 21 experimental runs, as listed in Table S1. To evaluate the significance of factors, their interactions, reliability and accuracy of the model, the experimental results were fitted to the quadratic model and analysis of variance (ANOVA) parameters (Table S2) including *P* and *F* values, lack-of-fit test, coefficients of determination ( $R^2$ ), adjusted  $R^2$ , adequate precision, standard deviation and coefficient of variation at a certain confidence level ( $\alpha = 0.05$ ) were considered. The factors with higher values of *F* and *P* values less than 0.05 have significant contribution to extraction recovery. Based on Table S2 and Fig. S2 (Pareto chart) A, B, C, D, AB, AD, BD, and  $A^2$  factors had the *P* values less than 0.05, which

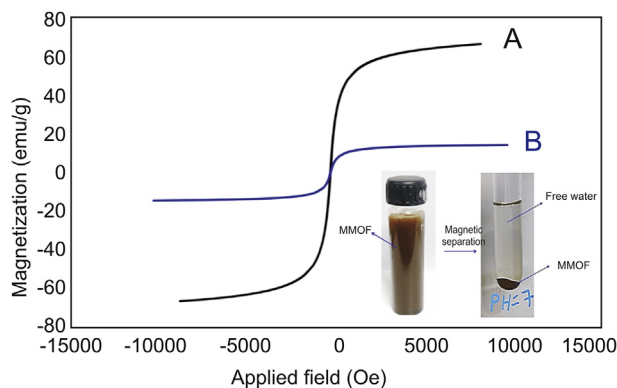


Fig. 6. VSM analysis of  $\text{Fe}_3\text{O}_4$  (A) and MMOF (B).

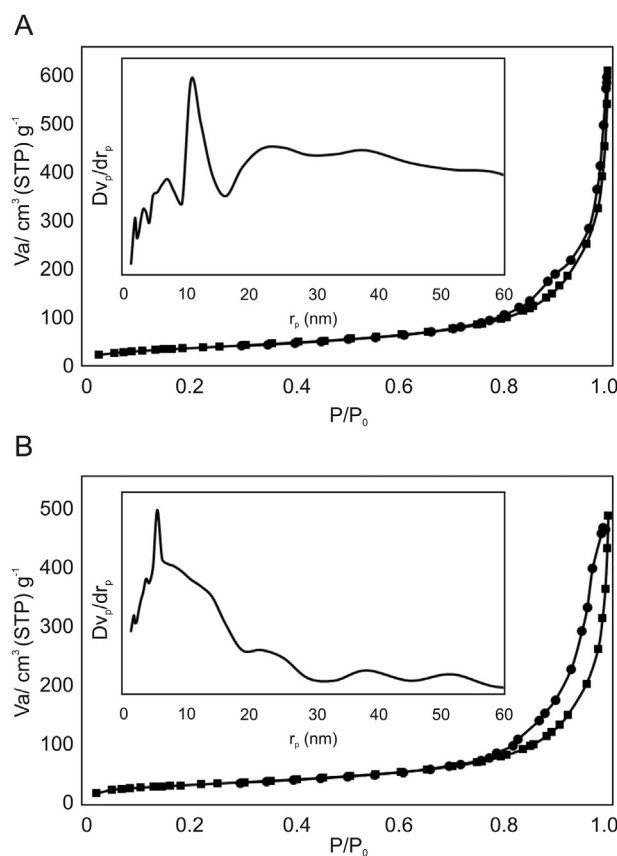


Fig. 7. The BET and pore size distribution analysis of MOF (A) and MMOF (B).

confirmed their significant contribution on extraction recovery while AC, BC, CD,  $B^2$ ,  $C^2$  and  $D^2$  factors had  $P$  values more than 0.05 that proved they were not significant and did not have significant contribution to extraction recovery. In addition, the lack-of-fit value higher than 0.05 (0.1028) and the correlation coefficient ( $R^2$ ) higher than 0.98 (0.9837) demonstrated the adequacy, reliability and fitness of the suggested model.  $R^2$  was calculated according to Eq. (1) and considered as a measure of the variation around the mean calculated by the model:

$$R^2 = 1 - \frac{SS_{\text{residual}}}{SS_{\text{model}} + SS_{\text{residual}}} \quad (1)$$

while adjusted  $R^2$  (0.9456) was determined using Eq. (2) and

applied as a measure of the variation around the mean determined through the experiments, adjusted for the number of terms in the model:

$$R_{\text{Adj}}^2 = 1 - \frac{SS_{\text{residual}}/DF_{\text{residual}}}{(SS_{\text{model}} + SS_{\text{residual}})/(DF_{\text{model}} + DF_{\text{residual}})} \quad (2)$$

Where  $SS$  and  $DF$  are the sum of squares and the degrees of freedom, respectively. Adequate precision represents the signal-to-noise ratio calculated based on Eq. (3) and had the value of 21.055 that confirmed a desirable adequate signal [33]:

$$\text{Adequate precision} = \frac{\max(\hat{y}) - \min(\hat{y})}{\sqrt{\bar{V}(\hat{y})}} \quad (3)$$

$$\bar{V}(\hat{y}) = \frac{1}{n} \sum_{i=1}^n V(\hat{y}) = \frac{P\sigma^2}{n} \quad (4)$$

Where  $\hat{y}$  is the response predicted by the model,  $P$  is the number of parameters applied in the model,  $\sigma^2$  is the residual mean square, and  $n$  is the number of experiments. The standard deviation and coefficient of variation of model were obtained to be 2.70 and 3.28, respectively, which shows the adequacy and reliability of the proposed model. Fig. S3 Shows good agreement between experimental extraction recovery (ER (%)) and calculated values. A second-order polynomial Eq. (5) was used to express response as a function of the independent variables as follows:

$$Y = \beta_0 + \sum_{i=1}^n \beta_i X_i + \sum_{i=1}^n \beta_{ii} X_i^2 + \sum_{i < j=1}^n \beta_{ij} X_i X_j + \epsilon \quad (5)$$

where  $\beta_0$  is the constant terms,  $\beta_i$ ,  $\beta_{ii}$  and  $\beta_{ij}$  are the regression coefficients for intercept, linear, quadratic and interaction terms, respectively;  $X_i$  and  $X_j$  are the independent variables and  $\epsilon$  is the residual associated to the experiments. The polynomial function allows to predict the value of the response  $Y$  based on specific values of the selected factors. Eq. (6) shows the effect of factors and their influences on ER (%) of AMP.

$$\begin{aligned} \text{AMP}_{\text{ER}(\%)} = & 83.00 + 12.00A + 6.75B + 4.72C + 5.75D + 3.69AB \\ & + 3.81AD + 6.56BD - 1.91A^2 \end{aligned} \quad (6)$$

Equation (6) represents the appropriate relation between ER (%), factors, their interactions and also quadratic model in which the coefficients show the intensity of each factor on ER (%). In addition, the positive signs show the growth of ER (%) while negative signs have an opposite effect and show decrease of ER (%). In the following part, to investigate the simultaneous effect of factors on ER (%), RSM 3D plots were applied. Fig. S4A shows the interaction between sorbent dosage and an ultrasonic time in which concurrent increase of them enhances ER (%). Increase of sorbent dosage enhances the specific surface area and available sites of MMOF which enhances the adsorption of AMP molecules onto MMOF and subsequently increase ER (%). In addition, an ultrasonic irradiation can enhance the dispersion of sorbent in sample solution and increase the contact between AMP molecules and MMOF. An adequate ultrasonic time increases mass transfer of AMP molecules from sample solution to MMOF surface, while high ultrasonic time might have an opposite effect and cause desorption of AMP molecules from MMOF surface which decreases ER (%). As the cow milk samples contain interfering species and accumulated matrix interferences, it is necessary to remove them from sample matrix.

Therefore, an adequate volume of washing solvent can remove impurities and enhance ER (%). The effect of washing solvent volume was assessed in the range of 1.5–3.5 mL. As shown in Figs. S4B, D, and F, an adequate volume of washing solvent can remove impurities while an inadequate volume of washings solvent may not be able to eliminate impurities from the sample. In addition, high volume of washing solvent not only can remove impurities, but also can remove AMP molecules from sample matrix. Figs. S4C, E and F represent the effect of eluent solvent volume on ER (%). The appropriate volume of eluent solvent can successfully elute the adsorbed AMP molecules from the MMOF surface. The effect of eluent solvent volume was investigated in the range of 1.5–3.5 mL and the best ER (%) was achieved in 2.0 mL of eluent solvent. Actually, 2.0 mL of eluent solvent was enough to desorb AMP molecules from cow milk samples. After RSM evaluation, for concurrent optimization of the analyzed factors, desirability function (DF) was applied based on Eq.(7) [34]:

$$DF = \frac{(\text{calculated } y_i - \text{minimum } y_i)}{(\text{maximum } y_i - \text{minimum } y_i)} \quad (7)$$

DF is a useful and conventional approach to determine the global optimum conditions which can convert the predicted and experimental response of each factor into a desirability score whereas it takes values between 0.0 and 1.0, which shows the completely undesirable and fully desired response, respectively. On the basis of the desirability score of 0.89, maximum recovery (92.9%) was achieved at optimum conditions set as the sorbent dosage (30 mg), ultrasonic irradiation (4.0 min), washing solvent volume (3.0 mL), and eluent solvent volume (2.0 mL) (Fig. S5).

#### 3.4. Evaluation of adsorption isotherms for determination of AMP by MMOF

Adsorption isotherm is an important aspect in adsorption study which shows the affinity, tendency as well as adsorption mechanism of analyte toward sorbent [35]. To determine the adsorption isotherms of AMP onto MMOF, the quantitative analysis was done in the concentration range of 5.0–50.0 mg/L of AMP. To estimate the binding properties of MMOF, different isotherm models including Langmuir, Freundlich, Temkin and Dubinin–Radushkevich were evaluated as listed in Table S3. According to Table S3,  $q_e$  shows the adsorbed AMP at equilibrium,  $Q_m$  and  $Q_s$  are the maximum adsorption capacity,  $C_e$  is the AMP concentration in sample solution at equilibrium,  $K_L$ ,  $R_L$ ,  $\alpha$ ,  $m$ ,  $B$ ,  $K_T$  and  $\beta$  are the Langmuir, Freundlich, Temkin and Dubinin–Radushkevich constants, respectively. Based on Table S3,  $Q_m$  for Langmuir model was achieved to be 250.5 mg/g and it is close to the value obtained from experimental results. The  $R^2$  for Langmuir model (0.9987) was higher than that for other models, which confirms that the adsorption of AMP onto MMOF can be well described by Langmuir isotherm. The principle of Langmuir isotherm is based on the monolayer adsorption of AMP molecules onto homogenous surface of sorbent while Freundlich model assumes the multilayer adsorption of AMP molecules onto heterogeneous surface of sorbent [36]. Considering the previous discussion on effect of pH, it is speculated that the AMP molecules are monolayer adsorbed on the surface of MMOF mainly through hydrogen bonding.  $R_L$  is a separation factor that can take values between 0 and 1, which show desired (irreversible) and undesired (reversible) adsorption, respectively. The  $R_L$  for AMP adsorption onto MMOFs was achieved to be 0.032–0.252 that is close to 0 and shows a desired (irreversible adsorption) process.  $m$  and  $B$  are the adsorption intensity and Temkin constant, respectively. Dubinin–Radushkevich isotherm represents the physical and/or chemical nature of adsorption [37]. If  $\beta$  values are between 8 and 16 kJ/mol, chemical

mechanisms control the adsorption process while for  $\beta$  lower than 8 kJ/mol, the adsorption process occurs through a physical mechanism [38]. The obtained  $\beta$  value was 7 kJ/mol, which confirms the physical adsorption of AMP onto MMOFs.

#### 3.5. Adsorption kinetic investigation for adsorption of AMP by MMOF

To examine the dynamics of adsorption process in terms of the order of rate constant, different adsorption kinetics such as First-order-kinetic, Pseudo-second-order-kinetic, Intraparticle diffusion and Elovich were studied. Based on Table S4,  $q_e$  and  $q_t$  are the adsorbed AMP at equilibrium and time  $t$ ,  $K_1$ ,  $K_2$ ,  $K_{diff}$ ,  $C$ ,  $\beta$  and  $\alpha$  are the constants of models, respectively [39]. According to Table S4,  $R^2$  value for Pseudo-second-order-kinetic model (0.9932) was higher than that for other models, which confirms adsorption kinetic followed by Pseudo-second-order. Also, the theoretical  $q_{e(cal)}$  (42.70) value was close to the experimental  $q_{e(exp)}$  (38.74) value for Pseudo-second-order-kinetic model, which indicates that the second order model is in good agreement with experimental data and can be used to favorably explain the AMP adsorption on MMOF.

#### 3.6. Method validation and real sample analysis

The developed MMOF-MSPE-HPLC/UV was fully validated under the optimum conditions in terms of the analytical figures of merit including linear range, limit of detection (LOD), limit of quantification (LOQ), precision, and accuracy. The calibration curve was constructed by plotting peak area versus AMP concentration in the wide range of 1.0–5000.0  $\mu\text{g/L}$  for AMP, for cow milk samples with satisfactory correlation coefficient ( $\geq 0.99$ ). The LOD and LOQ values were achieved to be 0.29  $\mu\text{g/L}$  and 0.96  $\mu\text{g/L}$  using  $3\sigma/\text{slope}$  and  $10\sigma/\text{slope}$  ratios, respectively, where  $\sigma$  is the standard deviation in the mean value for chromatograms obtained from the blank cow milk sample according to IUPAC recommendation [40]. The precision of the method was investigated by performing replicate analyses of blank cow milk samples at five different concentration levels (1.0, 10.0, 100.0, 1000.0 and 5000.0  $\mu\text{g/L}$ ) on the same day and in the six successive days expressed as relative standard deviation (RSD). As seen in Table 1, the RSD values were lower than 5.5% for all intra- and inter-day precision while supreme extraction recoveries (higher than 93.0%) were achieved, demonstrating qualified reproducibility and high accuracy of the proposed method. In order to indicate the effect of sample pretreatment in AMP analysis, the cow milk samples were directly injected to the HPLC. As shown in Fig. 8, due to the complexity of the cow milk samples, AMP peak was not detected, which indicated direct analysis of AMP is impossible. More excitingly, owing to the high potential of MMOF-MSPE for enriching AMP, trace quantities of AMP have remarkable signal. Consequently, the developed MMOF-MSPE is worthy for pre-concentration of AMP from complicating cow milk samples at trace level. In order to confirm the analytical applicability of the proposed method, the quantitative analysis of AMP in two different cow milk samples was carried out. The standard addition method was performed by spiking standard solution of AMP to the samples. As listed in Table 2, the accuracy were estimated through investigation of the recovery test. The ER% was found to be in the range of 95.0%–100.8% while RSD values were lower than 4.0% for triplicate continuous injections. These results suggest that the authoritative MMOF-MSPE-HPLC/UV method was mighty for clean extraction of AMP at trace level from intricate cow milk samples with supreme precision and accuracy.

#### 3.7. Selectivity of the proposed method

The effects of interfering compounds on the extraction and pre-

concentration of AMP in real samples were examined. Experiments performed using a 500 µg/L of AMP solution was performed in the presence of different concentrations of the interfering compounds (Table S5). In this study, the tolerance limit was defined as the highest amount of interfering compounds that lead to an error that is  $\pm 5.0\%$  in the determination of AMP. The results in Table S5 indicated that the presence of most of the metal ions did not interfere with the extraction and pre-concentration of trace quantities of AMP. On the other hand, due to similarity of AMP with some compounds such as amoxicillin and oxacillin, they interfered in extraction of AMP. This fact can be related to the structures and interactions between compounds and MMOF.

### 3.8. Reusability of the prepared MMOF

To examine the applicability of the proposed sorbent, the reusability aspect of sorbent was evaluated. For this purpose, different adsorption-desorption replications of MMOF were completed and results showed that the sorbent was applicable for at least eight times (Fig. S6). Thus, the proposed MMOF is not only ease of synthesis, inexpensive, and simple but also is a good candidate for practical application for extraction and determination of AMP from complicated cow milk samples.

### 3.9. Method comparison

The developed method was compared with those in some other reports for determination of AMP in different real samples. The MMOF in the present study showed the highest adsorption capacity (250.5 mg/g) and the short adsorption equilibrium time (4 min) and outstanding reusability (8 times). In addition, because of desirable magnetic properties (15 emu/g), it is easier to separate sorbent from sample and realize recycling than nonmagnetic MOF. From the analytical aspect, the linear range and LOD of the proposed method were approximately the same or better than those of some other methods, which represents the promising future of our present MMOF for determination of AMP from complicated cow milk samples [3,41–43] (Table 3). Moreover, the prepared MMOF was compared with some commercial sorbents presented in Table 4 [44–54]. These sorbents have been applied for determination of different compounds. The presented method has exclusive properties in terms of high adsorption capacity and short extraction time which are better than those of some reported sorbents. Preparation of the proposed sorbent is easy, simple and cheap compared to some reported methods. The proposed method does not need an expensive equipment and the materials and reagents are available. Some reported methods are multi-step and time consuming while the presented method is one step.

**Table 1**

Intra-day and inter-day precision and recovery of the MMOF-MSPE-HPLC/UV method for ampicillin determination in spiked cow milk samples ( $n = 5$ ).

Analyte	Added (µg/L)	Found (µg/L) $\pm$ SD	RSD (%)	Recovery (%)
AMP (Intra-day)	1.0	0.98 $\pm$ 0.05	4.7	98.0
	10.0	9.84 $\pm$ 0.10	2.7	98.4
	100.0	101.4 $\pm$ 2.40	2.3	101.4
	1000.0	990.0 $\pm$ 16.8	1.7	99.0
	5000.0	5050.0 $\pm$ 82.8	1.6	101.0
AMP (Inter-day)	1.0	0.94 $\pm$ 0.04	5.3	94.0
	10.0	9.82 $\pm$ 0.28	2.9	98.2
	100.0	98.6 $\pm$ 2.1	2.1	98.6
	1000.0	985.4 $\pm$ 21.9	2.2	98.5
	5000.0	4936.0 $\pm$ 114.6	2.3	98.7

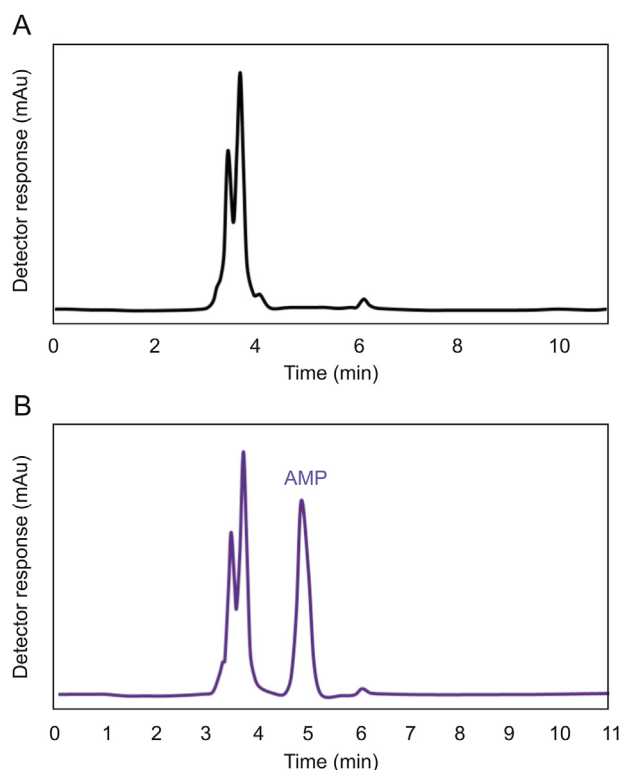


**Fig. 8.** Typical chromatograms of (A) direct injection of extracted cow milk sample and (B) spiked cow milk sample after MMOF-MSPE procedure.

**Table 2**

Accuracy of the MMOF-MSPE-HPLC/UV method ( $n = 5$ ).

Sample	Added (µg/L)	Found (µg/L) $\pm$ SD	RSD (%)	Recovery (%)
Cow milk sample 1	0.0	ND	–	–
	10.0	9.84 $\pm$ 0.2	2.1	98.4
	100.0	95.0 $\pm$ 2.6	2.8	95.0
	1000.0	991.0 $\pm$ 15.0	1.5	99.1
Cow milk sample 2	0.0	ND	–	–
	10.0	9.72 $\pm$ 0.4	3.8	97.2
	100.0	98.0 $\pm$ 2.3	2.3	98.0
	1000.0	1008.0 $\pm$ 13.0	1.3	100.8

ND=Not detect.

## 4. Conclusion

In the present study, we prepared MMOF material by a simple and facile one pot solvothermal method and successfully applied it for the determination of AMP from cow milk samples for the first time. Compared to some reported sorbents, the proposed sorbent has high adsorption capacity and (250.5 mg/g) and also short extraction time (4 min). The magnetic property of the prepared sorbent makes it easy to separate sorbent from sample solution, which not only reduces extraction time but also improves the repeatability of sorbent. The MMOF material could be effectively regenerated by recycling it over 8 times. Under the optimized conditions, the proposed method is applicable for linear range of 1.0–5000.0 µg/L with detection limit of 0.29 µg/L, satisfactory recoveries ( $\geq 95.0\%$ ) and acceptable repeatability (RSD less than 4.0%). Compared to methods that have been used for determination of AMP, the presented work represents the satisfactory results in terms of synthesis of sorbent and analytical aspect. In view of the combined advantages of magnetic Fe<sub>3</sub>O<sub>4</sub> and MOF, we could foresee

**Table 3**  
Comparison between MMOF-MSPE-HPLC/UV and other approaches for determination of ampicillin.

Sample	Sample preparation method	Sorbent	Adsorption capacity (mg/g)	Equilibrium time (min)	Detection method	Linear range (µg/L)	Recovery (%)	LOD (µg/L)	LOQ (µg/L)	RSD (%)	References
Urine samples	LSP <sup>a</sup>	SNPs <sup>b</sup>	–	–	Colorimetric	25.0–1200.0	–	10.0	–	< 5.0	[3]
Food samples	SPE	MIP <sup>c</sup>	–	–	Spectrofluorimetry	25.0–100.0	81.7–98.7	0.05	0.12	< 3.2	[41]
Milk and blood	SPE	MIP	18.2	10	HPLC-UV	5.0–200	92.1–107.6	0.05	0.2	<5.0	[42]
Cow milk samples	SPE	MIP	–	–	HPLC-UV	100.0–500.0	≥95	10.7	35.8	<7.0	[43]
Cow milk samples	MSPE	MMOFs	250.5	5.0	HPLC-UV	1.0–5000	95.0–100.8	0.29	0.96	< 4.0	Present work

<sup>a</sup> Localized surface plasmon resonance.

<sup>b</sup> Silver nanoparticles.

<sup>c</sup> Molecularly imprinted polymer.

**Table 4**  
Comparison of the prepared MMOF with some commercial sorbents.

Sorbent	Extraction time (min)	Adsorption capacity (mg/g)	Linear range (µg/L)	LOD (µg/L)	RSD (%)	References
MMNCZ <sup>a</sup>	3.5	–	2.0–150.0	0.93–1.08	2.13–2.78	[45]
MPC <sub>18</sub> <sup>b</sup>	60	–	20–1000	6.90–9.52	4.1–9.2	[46]
CPF <sup>c</sup>	30	–	0.05–5.00	0.0004–0.0044	–	[47]
MS <sup>d</sup>	15	–	6–10000	1.4	<6	[48]
L-CMZ <sup>e</sup>	–	0.6	0.1–7.5	0.04	1.4	[49]
C <sub>18</sub> composite	60	–	0.002–0.5	0.000059–0.000151	4.3–10.2	[44]
CMZN <sup>f</sup>	2	–	4–24000	4–4000	6.2–12.9	[50]
Activated carbon	–	30.5	0.1–200	0.006	1.26	[51]
CGOPC <sup>g</sup>	10	–	50–10000	3.7–7.1	1.2–6.4	[52]
ACC <sub>18</sub> F <sup>h</sup>	40	–	1–500	0.549–0.673	≤13.5	[53]
CBP <sup>i</sup>	8	–	1–4000	–	<10	[54]
MMOF	4	250.5	1–5000	0.29	<4	This work

<sup>a</sup> Modified magnetic natural clinoptilolite zeolite.

<sup>b</sup> Membrane protected C<sub>18</sub>.

<sup>c</sup> Commercial polymeric fiber.

<sup>d</sup> Mesoporous silica.

<sup>e</sup> L-cystine modified zeolite.

<sup>f</sup> CTAB modified zeolite NaY.

<sup>g</sup> Carboxylated graphene oxide/polyvinyl chloride.

<sup>h</sup> Agarose-chitosan-C<sub>18</sub> film.

<sup>i</sup> Cyclodextrin based polymer.

that this magnetic adsorbent will have great potential for determination of AMP from cow milk samples.

### Conflicts of interest

The authors declare that there are no conflicts of interest.

### Acknowledgments

This work was financially supported by Graduate School and Research Council of Yasouj University.

### Appendix A. Supplementary data

Supplementary data to this article can be found online at <https://doi.org/10.1016/j.jpha.2020.02.006>.

### References

- [1] K.E. Stępnik, I. Malinowska, M. Maciejewska, A new application of micellar liquid chromatography in the determination of free ampicillin concentration in the drug–human serum albumin standard solution in comparison with the adsorption method, *Talanta* 153 (2016) 1–7.
- [2] J. Wang, K. Ma, H. Yin, et al., Aptamer based voltammetric determination of ampicillin using a single-stranded DNA binding protein and DNA functionalized gold nanoparticles, *Microchim. Acta* 185 (2018) 68.
- [3] K. Shrivastava, J. Sahu, P. Maji, et al., Label-free selective detection of ampicillin drug in human urine samples using silver nanoparticles as a colorimetric sensing probe, *New J. Chem.* 41 (2017) 6685–6692.
- [4] X. Wu, X. Wang, W. Lu, et al., Water-compatible temperature and magnetic dual-responsive molecularly imprinted polymers for recognition and extraction of bisphenol A, *J. Chromatogr. A* 1435 (2016) 30–38.
- [5] M. Zhang, J. Yang, X. Geng, et al., Magnetic adsorbent based on mesoporous silica nanoparticles for magnetic solid phase extraction of pyrethroid pesticides in water samples, *J. Chromatogr. A* 1598 (2019) 20–29.
- [6] H. Li, W. Han, R. Lv, et al., Dual-function mixed-lanthanide metal–organic framework for ratiometric water detection in bioethanol and temperature sensing, *Anal. Chem.* 91 (2019) 2148–2154.
- [7] S. Lin, Z. Song, G. Che, et al., Adsorption behavior of metal–organic frameworks for methylene blue from aqueous solution, *Microporous Mesoporous Mater.* 193 (2014) 27–34.
- [8] C. Petit, B. Mendoza, T.J. Bandoz, Reactive adsorption of ammonia on Cu-based MOF/graphene composites, *Langmuir* 26 (2010) 15302–15309.
- [9] A.R. Bagheri, M. Arabi, M. Ghaedi, et al., Dummy molecularly imprinted polymers based on a green synthesis strategy for magnetic solid-phase extraction of acrylamide in food samples, *Talanta* 195 (2019) 390–400.
- [10] M. Arabi, M. Ghaedi, A. Ostovan, Development of a lower toxic approach based on green synthesis of water-compatible molecularly imprinted nanoparticles for the extraction of hydrochlorothiazide from human urine, *ACS Sustain. Chem. Eng.* 5 (2017) 3775–3785.
- [11] A.R. Bagheri, M. Ghaedi, A. Asfaram, et al., Comparative study on ultrasonic assisted adsorption of dyes from single system onto Fe<sub>3</sub>O<sub>4</sub> magnetite nanoparticles loaded on activated carbon: experimental design methodology, *Ultrason. Sonochem.* 34 (2017) 294–304.
- [12] R.D.C. Soltani, Z. Miraftehi, M. Mahmoudi, et al., Stone cutting industry waste-supported zinc oxide nanostructures for ultrasonic assisted decomposition of

- an anti-inflammatory non-steroidal pharmaceutical compound, *Ultrason. Sonochem.* (2019) 104669.
- [13] A.R. Bagheri, M. Ghaedi, A. Asfaram, et al., Design and construction of nano-scale material for ultrasonic assisted adsorption of dyes: application of derivative spectrophotometry and experimental design methodology, *Ultrason. Sonochem.* 35 (2017) 112–123.
  - [14] Q. You, Y. Zhang, Q. Zhang, et al., High-capacity thermo-responsive magnetic molecularly imprinted polymers for selective extraction of curcuminoids, *J. Chromatogr. A* 1354 (2014) 1–8.
  - [15] A.R. Abbasi, M. Karimi, K. Daasbjerg, Efficient removal of crystal violet and methylene blue from wastewater by ultrasound nanoparticles Cu-MOF in comparison with mechanosynthesis method, *Ultrason. Sonochem.* 37 (2017) 182–191.
  - [16] A. Asfaram, M. Ghaedi, K. Dashtian, Rapid ultrasound-assisted magnetic microextraction of gallic acid from urine, plasma and water samples by HKUST-1-MOF-Fe<sub>3</sub>O<sub>4</sub>-GA-MIP-NPs: UV–vis detection and optimization study, *Ultrason. Sonochem.* 34 (2017) 561–570.
  - [17] S. Bao, L. Tang, K. Li, et al., Highly selective removal of Zn (II) ion from hot-dip galvanizing pickling waste with amino-functionalized Fe<sub>3</sub>O<sub>4</sub>@ SiO<sub>2</sub> magnetic nano-adsorbent, *J. Colloid Interface Sci.* 462 (2016) 235–242.
  - [18] R. Kaur, A. Kaur, A. Umar, et al., Metal organic framework (MOF) porous octahedral nanocrystals of Cu-BTC: synthesis, properties and enhanced adsorption properties, *Mater. Res. Bull.* 109 (2019) 124–133.
  - [19] K.Y.A. Lin, Y.T. Hsieh, Copper-based metal organic framework (MOF), HKUST-1, as an efficient adsorbent to remove p-nitrophenol from water, *J. Taiwan. Inst. Chem. Eng.* 50 (2015) 223–228.
  - [20] Z. Shi, C. Xu, H. Guan, et al., Magnetic metal organic frameworks (MOFs) composite for removal of lead and malachite green in wastewater, *Colloid. Surface.* 539 (2018) 382–390.
  - [21] L. Huang, M. He, B. Chen, et al., A mercapto functionalized magnetic Zr-MOF by solvent-assisted ligand exchange for Hg<sup>2+</sup> removal from water, *J. Mater. Chem.* 4 (2016) 5159–5166.
  - [22] K.H. Chu, Y.A.J. Al-Hamadani, C.M. Park, et al., Ultrasonic treatment of endocrine disrupting compounds, pharmaceuticals, and personal care products in water: a review, *Chem. Eng. J.* 327 (2017) 629–647.
  - [23] X.R. Shi, X.L. Chen, Y.L. Hao, et al., Magnetic metal-organic frameworks for fast and efficient solid-phase extraction of six Sudan dyes in tomato sauce, *J. Chromatogr. B* 1086 (2018) 146–152.
  - [24] S. Babić, A.J.M. Horvat, D. Mutavdžić Pavlović, et al., Determination of pKa values of active pharmaceutical ingredients, *TrAC Trends Anal. Chem.* 26 (2007) 1043–1061.
  - [25] A. Ostovan, M. Ghaedi, M. Arabi, et al., Hydrophilic multitemplate molecularly imprinted biopolymers based on a green synthesis strategy for determination of B-family vitamins, *ACS Appl. Mater. Interfaces* 10 (2018) 4140–4150.
  - [26] H. Gholami, M. Ghaedi, M. Arabi, et al., Application of molecularly imprinted biomembrane for advancement of matrix solid-phase dispersion for clean enrichment of parabens from powder sunscreen samples: optimization of chromatographic conditions and green approach, *ACS Omega* 4 (2019) 3839–3849.
  - [27] H. Gholami, M. Arabi, M. Ghaedi, et al., Column packing elimination in matrix solid phase dispersion by using water compatible magnetic molecularly imprinted polymer for recognition of melamine from milk samples, *J. Chromatogr. A* 1594 (2019) 13–22.
  - [28] H. Gholami, M. Ghaedi, A. Ostovan, et al., Preparation of hollow porous molecularly imprinted and aluminum(III) doped silica nanospheres for extraction of the drugs valsartan and losartan prior to their quantitation by HPLC, *Microchim. Acta* 186 (2019) 702.
  - [29] M. Arabi, M. Ghaedi, A. Ostovan, Development of dummy molecularly imprinted based on functionalized silica nanoparticles for determination of acrylamide in processed food by matrix solid phase dispersion, *Food Chem.* 210 (2016) 78–84.
  - [30] M. Arabi, M. Ghaedi, A. Ostovan, Water compatible molecularly imprinted nanoparticles as a restricted access material for extraction of hippuric acid, a biological indicator of toluene exposure, from human urine, *Microchim. Acta* 184 (2017) 879–887.
  - [31] A. Ostovan, M. Ghaedi, M. Arabi, et al., Hollow porous molecularly imprinted polymer for highly selective clean-up followed by influential preconcentration of ultra-trace glibenclamide from bio-fluid, *J. Chromatogr. A* 1520 (2017) 65–74.
  - [32] A.R. Bagheri, M. Ghaedi, Synthesis of chitosan based molecularly imprinted polymer for pipette-tip solid phase extraction of Rhodamine B from chili powder samples, *Int. J. Biol. Macromol.* 139 (2019) 40–48.
  - [33] M.K. Uddin, U. Baig, Synthesis of Co<sub>3</sub>O<sub>4</sub> nanoparticles and their performance towards methyl orange dye removal: characterisation, adsorption and response surface methodology, *J. Clean. Prod.* 211 (2019) 1141–1153.
  - [34] P.C. Bandara, E.T. Nades, D.F. Rodrigues, Use of response surface methodology to develop and optimize the composition of a chitosan-polyethyleneimine-graphene oxide nanocomposite membrane coating to more effectively remove Cr (VI) and Cu (II) from water, *ACS Appl. Mater. Interfaces* 11 (2019) 17784–17795.
  - [35] G. Sarma, S.S. Gupta, K. Bhattacharyya, Removal of hazardous basic dyes from aqueous solution by adsorption onto kaolinite and acid-treated kaolinite: kinetics, isotherm and mechanistic study, *SN Appl. Science* 1 (2019) 211.
  - [36] C.S. Araújo, I.L. Almeida, H.C. Rezende, et al., Elucidation of mechanism involved in adsorption of Pb (II) onto lobeira fruit (*Solanum lycocarpum*) using Langmuir, Freundlich and Temkin isotherms, *Microchim. J.* 137 (2018) 348–354.
  - [37] F.A. Razmi, N. Ngadi, S. Wong, et al., Kinetics, thermodynamics, isotherm and regeneration analysis of chitosan modified pandan adsorbent, *J. Clean. Prod.* 231 (2019) 98–109.
  - [38] D. Liu, P. Lopez-Sanchez, M. Martinez-Sanz, et al., Adsorption isotherm studies on the interaction between polyphenols and apple cell walls: effects of variety, heating and drying, *Food Chem.* 282 (2019) 58–66.
  - [39] H.R. Noormohamadi, M.R. Fat'hi, M. Ghaedi, Fabrication of polyethyleneimine modified cobalt ferrite as a new magnetic sorbent for the micro-solid phase extraction of tartrazine from food and water samples, *J. Colloid Interface Sci.* 531 (2018) 343–351.
  - [40] A.M. Committee, Recommendations for the definition, estimation and use of the detection limit, *Analyst* 112 (1987) 199–204.
  - [41] P. Raksawong, P. Nurerk, K. Chullasat, et al., A polypyrrole doped with fluorescent CdTe quantum dots and incorporated into molecularly imprinted silica for fluorometric determination of ampicillin, *Microchim. Acta* 186 (2019) 338.
  - [42] N. Wu, Z. Luo, Y. Ge, et al., A novel surface molecularly imprinted polymer as the solid-phase extraction adsorbent for the selective determination of ampicillin sodium in milk and blood samples, *J. Pharm. Anal.* 6 (2016) 157–164.
  - [43] B. Soledad-Rodríguez, P. Fernández-Hernando, R. Garcinuño-Martínez, et al., Effective determination of ampicillin in cow milk using a molecularly imprinted polymer as sorbent for sample preconcentration, *Food Chem.* 224 (2017) 432–438.
  - [44] S. Li, C. Lu, F. Zhu, et al., Preparation of C18 composite solid-phase micro-extraction fiber and its application to the determination of organochlorine pesticides in water samples, *Anal. Chim. Acta* 873 (2015) 57–62.
  - [45] T. Amiri-Yazani, R. Zare-Dorabi, M. Rabbani, et al., Highly efficient ultrasonic-assisted pre-concentration and simultaneous determination of trace amounts of Pb (II) and Cd (II) ions using modified magnetic natural clinoptilolite zeolite: response surface methodology, *Microchim. J.* 146 (2019) 498–508.
  - [46] X. Mao, M. He, B. Chen, et al., Membrane protected C18 coated stir bar sorptive extraction combined with high performance liquid chromatography-ultraviolet detection for the determination of non-steroidal anti-inflammatory drugs in water samples, *J. Chromatogr. A* 1472 (2016) 27–34.
  - [47] T.M. Hii, C. Basheer, H.K. Lee, Commercial polymeric fiber as sorbent for solid-phase microextraction combined with high-performance liquid chromatography for the determination of polycyclic aromatic hydrocarbons in water, *J. Chromatogr. A* 1216 (2009) 7520–7526.
  - [48] F. Momtazan, S. Khodadoust, F. Zeraatpishe, et al., Synthesis of mesoporous silica for adsorption of chlordiazepoxide and its determination by HPLC: experimental design, *J. Separ. Sci.* 42 (2019) 3253–3260.
  - [49] S.A. Rezvani, A. Soleymanpour, Application of l-cystine modified zeolite for preconcentration and determination of ultra-trace levels of cadmium by flame atomic absorption spectrometry, *J. Chromatogr. A* 1436 (2016) 34–41.
  - [50] P. Salisaeng, P. Arnnok, N. Patdhanagul, et al., Vortex-assisted dispersive micro-solid phase extraction using CTAB-modified zeolite NaY sorbent coupled with HPLC for the determination of carbamate insecticides, *J. Agric. Food Chem.* 64 (2016) 2145–2152.
  - [51] B. Feist, Comparison of the sorption capacities of 1, 10-phenanthroline and 2, 2-bipyridyl complexes with cadmium on activated carbon and graphene oxide, *Microchim. J.* 145 (2019) 588–595.
  - [52] Z. Zhong, G. Li, Z. Luo, et al., Carboxylated graphene oxide/polyvinyl chloride as solid-phase extraction sorbent combined with ion chromatography for the determination of sulfonamides in cosmetics, *Anal. Chim. Acta* 888 (2015) 75–84.
  - [53] N.T. Ng, M.M. Sanagi, W.N.W. Ibrahim, et al., Agarose-chitosan-C18 film micro-solid phase extraction combined with high performance liquid chromatography for the determination of phenanthrene and pyrene in chrysanthemum tea samples, *Food Chem.* 222 (2017) 28–34.
  - [54] N.A. Manaf, B. Saad, M.H. Mohamed, et al., Cyclodextrin based polymer sorbents for micro-solid phase extraction followed by liquid chromatography tandem mass spectrometry in determination of endogenous steroids, *J. Chromatogr. A* 1543 (2018) 23–33.